Received 22 November 2022; revised 13 December 2022; accepted 29 December 2022. Date of publication 9 January 2023; date of current version 20 January 2023.

Digital Object Identifier 10.1109/OJCOMS.2023.3234981

Three-User Cooperative Dual-Stage Non-Orthogonal Multiple Access for Power Line Communications

ROOPESH RAMESH [1] (Graduate Student Member, IEEE), SANJEEV GURUGOPINATH [1] (Senior Member, IEEE), AND SAMI MUHAIDAT [2] (Senior Member, IEEE)

[1]Department of Electronics and Communication Engineering, PES University, Bengaluru 560085, India

[2]Center for Cyber-Physical Systems and the Department of Electrical and Computer Engineering, Khalifa University, Abu Dhabi, UAE

CORRESPONDING AUTHOR: S. MUHAIDAT (e-mail: sami.muhaidat@ku.ac.ae).

ABSTRACT We present a cooperative, dual-stage (DS) non-orthogonal multiple access (NOMA) scheme for power line communication (PLC) systems, where three PLC modems are served in two time slots. The network consists of a source (S) modem, two relay (R) modems and a destination (D) modem. In each of the two time slots, S communicates with one R using NOMA, and the other R communicates with D using the decode-and-forward technique. We consider both scenarios where a direct link may or may not exist between S and D. We derive expressions for the approximate average sum rate and overall outage probability of the network. Next, we formulate an optimization problem to find the optimal power allocation coefficients at S, such that the sum rate is maximized. We establish the accuracy of our approximations using Monte Carlo simulations. Furthermore, we show that our scheme outperforms the two-user single-stage and the DS schemes, and the three-user NOMA scheme proposed in the earlier literature, in terms of sum rate and outage probability.

INDEX TERMS Cooperative power line communication, dual-stage, non-orthogonal multiple access, outage probability, sum rate.

I. INTRODUCTION

POWER line communication (PLC) technology uses the existing infrastructure of power distribution networks for information transfer, which results in low deployment costs and a better performance compared to wireless technologies [1]. Some of the limitations and key issues for information transmission over a PLC channel includes the effects due to selective multipath fading, receiver noise and electromagnetic interference. Majority of PLC channel impairments due to the harsh conditions are characterized due to these impairments. Different models for signal impairments in a PLC channel have been proposed in the literature [2], [3]. Among these models, the lognormal distribution best describes the random effects due to unmatched loads observed in PLC network topologies and branches [4]. Among the noise models, a mixture of the impulsive component and the background component, for which a Bernoulli-Gaussian distribution is employed, which is amenable to analysis and captures the effect of the mixture of components [5], [6]. There has been a considerable research attention on PLC from both academia and industry recently, owing to features such as reliability and security, apart from those mentioned above [7]. Cooperative PLC has also emerged as a promising technology for applications in beyond 5G and Internet-of-Things [8]. In conventional cooperation relay based on orthogonal multiple access (OMA) schemes, such as time division multiplexing, the signal received from relay and transmitter over the two time slots is combined at the receiver [9]. This leads to an improved performance at the receiver, at the expense of spectral efficiency.

The recent surge in literature on non-orthogonal multiple access (NOMA) indicates its potential in next generation communication systems [10], [11], [12], [13]. In NOMA, multiple users are served simultaneously over same time and frequency resources, by appropriately multiplexing the transmitted signals either in code-domain or power-domain. The user symbols are assigned different transmit power levels

based on the user channel conditions. User with the best channel is allocated with least power, while the user with the worst channel is allocated highest power. Additionally, successive interference cancellation (SIC) is employed at the receiver, while superposition coding is used at the transmitter. Given these advantages, NOMA was proposed for cooperative PLC, which yields a higher spectral efficiency and lower latency than OMA [12], [14]. Most of the existing literature on NOMA for cooperative PLC has considered two-user networks. In [12], the authors proposed a single stage (SS) NOMA-based dual-hop decode-and-forward DF cooperative relaying scheme for narrowband PLC. The transmitter modem sends a superimposed signal to two receiver modems in first time slot. One of the receivers acts as a relay to the other, which decodes the symbols using successive interference cancellation (SIC), and assists the other node by transmitting its symbol again in the second slot. This idea was further investigated in [15], where a dual stage (DS) setup was considered, which was shown to outperform the SS case. More recently, the authors in [11] studied the outage probability performance of NOMA-PLC considering both SS and DS schemes. Furthermore, there are studies with different setups in a two-user NOMA for a hybrid wireless-PLC network [16], [17]. In particular, the authors in [16] studied the outage probability and sum rate considering DS scheme under the additive white Gaussian and Bernoulli-Gaussian noises. The source modem sends a superimposed signal to relay in the first time slot. The relay forwards the superimposed signals to both destination modems in the second slot. However, the aforementioned studies do not consider either sum rate or outage probability performance study of a three-user PLC network, under Bernoulli-Gaussian noise. The performance of three-user NOMA schemes for wireless communication were studied in [18] and [19], where the authors showed that NOMA outperforms OMA, in terms of the overall network sum rate. However, none of these works consider PLC networks. To the best of the authors' knowledge, performance of SS or DS schemes in NOMA-PLC networks with three users has not been considered in the literature.

The contributions of this paper in relation to the existing literature are as follows.

- We investigate the three-user cooperative NOMA scheme proposed for wireless networks in [19] in the context of PLC, and study its performance in terms of outage probability and network sum rate.
- We derive expressions for approximate sum rate and outage probability of the considered PLC network, in two scenarios – without and with a direct link between the source and destination modems. Additionally, we establish the tightness of our approximations through Monte Carlo simulations.
- Furthermore, we formulate an optimization problem and propose a solution to find the optimal power coefficients for NOMA at the source that maximizes the network sum rate.

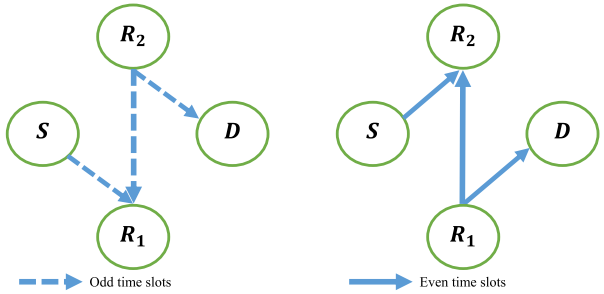

FIGURE 1. Cooperative NOMA for a PLC system (without direct link to D) with three receiver modems, with operation of the source and receiver modems at (a) odd (left) and (b) even (right) time slots, respectively.

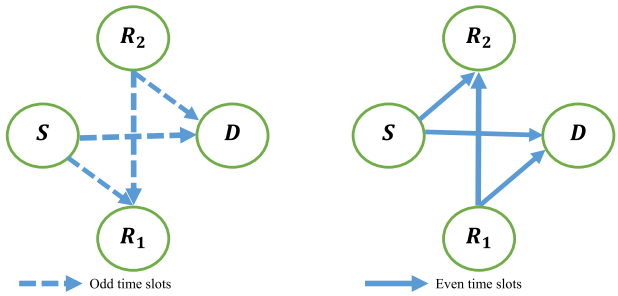

FIGURE 2. Cooperative NOMA for a PLC system (with a direct link to D) with three receiver modems, with operation of the source and receiver modems at (a) odd (left) and (b) even (right) time slots, respectively.

- In terms of sum rate, we show that the considered scheme outperforms the three-user NOMA scheme considered in [18] extended to PLC, and the SS and DS two-user NOMA schemes in [15].
- Moreover, in terms of outage probability, we show that our proposed scheme outperforms the SS and DS two-user NOMA schemes in [11].

The rest of the paper is organized as follows. Section II describes the system model of the considered three-user PLC network. In Section III, analytical expressions are derived for the average sum rates without and with a direct link between the source and destination modems. The corresponding outage probabilities are derived in Section IV. Validation of our analysis is presented in Section V. Concluding remarks are presented in Section VI. The notations used in this paper are given in Table 1.

II. SYSTEM MODEL

Consider a three user power line communication (PLC) setup which consists of a source (S) modem and three receiver modems, as shown in Figs. 1 and 2. All modems operate in half-duplex mode. Out of the three receiver modems, two modems, namely R_1 and R_2 are closer to S with a direct link between S-R_1 and S-R_2. The third modem D is far from S, and may not or may share a direct link with S, as shown in Fig. 1 and Fig. 2, respectively [19], [20]. The channel gains between S-D, S-R_1, S-R_2, R_1-D, R_2-D and R_1-R_2, denoted by h_{SD}, h_{SR_1}, h_{SR_2}, h_{R_1D}, h_{R_2D}, and $h_{R_1R_2}$,

TABLE 1. Table of notations.

Symbol	Description
S, R_1, R_2, D	Source, relay-1, relay-2 and destination modems
k	Index for modems, $i \in \{S, R_1, R_2, D\}$
$s_1(t), s_2(t), s_3(t)$	Symbols indented to R_1, R_2, D, at time t
$\hat{s_3}(t)$	Estimate of $s_3(t)$ from the previous time slot
i	Index for communication links, for $i \in \{SD, SR_1, SR_2, R_1D, R_2D, R_1R_2\}$
h_i	Channel gains for each link i
A_i	Attenuation factor in each link i
d_i	Distance between the nodes in each link i
σ^2	Noise variance, including impulsive component
$\gamma_{R_1}, \gamma_{R_2}$	SINR at R_1 and R_2, respectively
$\gamma_{D,i}$	SINR at D, due to signal received from link i
C_i	Capacity of link i
C_{sum}	Average sum rate of the network
$P_{\text{out}}^{(R_1)}, P_{\text{out}}^{(R_2)}$	Outage probability at R_1 and R_2, respectively
$P_{\text{out}}^{(R_2)}$	Outage probability at R_2
$P_{\text{out}}^{(D)}$	Outage probability at D, without direct link
$P_{\text{out}}^{(SD)}$	Outage probability at D, with direct link
P_{out}	Overall outage probability
$\alpha_\ell \triangleq 2^{2r_\ell} - 1$	Threshold rates for outage due to symbols $\ell \in \{s_1, s_2, s_3\}$

respectively, are modeled as independent lognormal random variables [4]. The lognormal fading model is widely employed in PLC systems, which captures the statistics due to the network topology load mismatch and the signal propagation in network branches [21]. The probability density function (PDF) of these channel gains is given by

$$f(h_i) = \frac{1}{\sqrt{2\pi}\sigma_i h_i} \exp\left[-\frac{(\log h_i - \mu_i)^2}{2\sigma_i^2}\right] \tag{1}$$

for $i \in \{SD, SR_1, SR_2, R_1D, R_2D, R_1R_2\}$. Parameters μ_i and σ_i^2 denote the mean and the variance of $10\log_{10}(h_i)$, $i \in \{SD, SR_1, SR_2, R_1D, R_2D, R_1R_2\}$, respectively. We use the notation $h_i \sim \mathcal{LN}(\mu_i, \sigma_i^2)$ to denote the above described PDF. Additionally, we consider the impairments due to distance- and frequency-dependencies in the attenuation, which are denoted by $A_i(d_i, f)$ for $i \in \{SD, SR_1, SR_2, R_1D, R_2D, R_1R_2\}$ respectively, where f denotes the frequency of communication and d_i denotes the distances between the nodes $i \in \{SD, SR_1, SR_2, R_1D, R_2D, R_1R_2\}$. Let P_S denote the total power available at S. Information transmission from S occurs over two time slots, namely the even- and odd-numbered slots. In each time slot, S uses non-orthogonal multiple access (NOMA) to transmit two symbols to either R_1 or R_2, which will be explained in detail next.

A. ODD TIME SLOTS

During the odd time slot $(2t+1), t = 0, 1, \ldots,$ S transmits the superimposed signal

$$x_s(2t+1) = \left(\sqrt{\beta_1 P_S} s_1(2t+1) + \sqrt{\beta_2 P_S} s_3(2t+1)\right), \tag{2}$$

to R_1, where $s_1(2t+1)$ and $s_3(2t+1)$ are the signals intended to R_1 and D, respectively. Parameters β_1 and β_2 are the power allocation coefficients for R_1 and D, respectively, such that $\beta_2 > \beta_1 \geq 0$ and $\beta_1 + \beta_2 = 1$. In an odd time slot $2t+1$, R_2 also acts as a relay and forwards the decoded signal s_3 to R_1 and D. As will be shown later in (18), R_2 would receive superimposed signals from S and R_1 at the previous even slot $2t$. Assuming that signals from S are successfully decoded, signal transmitted by R_2 is given by

$$x_{R_2}(2t+1) = \sqrt{P_{R_2}}\hat{s}_3(2t), \tag{3}$$

where P_{R_2} is the transmit power of R_2, and $\hat{s}_3(2t)$ denotes the signal destined for D, which was correctly detected by R_2. Following this, the received signal at R_1 is given by

$$\begin{aligned} z_{R_1}(2t+1) = {} & A_{SR_1}(d_{SR_1}, f) h_{SR_1} x_s(2t+1) \\ & + A_{R_2R_1}(d_{R_2R_1}, f) h_{R_2R_1} x_{R_2}(2t+1) + n_{R_1}(2t+1), \end{aligned} \tag{4}$$

where $n_k(2t+1), k = R_1, D$ represents the receiver noise random variables which are modeled by independent Bernoulli-Gaussian random variables with PDF [5],

$$f_{(n_k)}(x) = (1-p)\, f_B(x) + p\, f_I(x). \tag{5}$$

Here, $f_B(x)$ denotes the PDF for the background noise, which is the additive white Gaussian noise (AWGN) with zero mean and variance σ_B^2, and $f_I(x)$ denotes the PDF for the impulsive component. For the ease of analysis, we let $f_I(x)$ to be another independent Gaussian distribution with zero mean and variance σ_I^2. Also, $0 \leq p < 1$ is the probability of the occurrence of the impulsive component. As a consequence, the variance of $n_k(2t+1)$ is given by

$$\sigma^2 = \sigma_B^2(1+K),$$

where $K = \sigma_I^2/\sigma_B^2$ is the impulsive noise index. Typically, $K \in [10, 100]$ [6]. The received signal at R_1 is obtained by substituting (2) and (3) into (4) as

$$\begin{aligned} z_{R_1}(2t+1) = {} & \sqrt{\beta_1 P_S} A_{SR_1}(d_{SR_1}, f) h_{SR_1} s_1(2t+1) \\ & + \sqrt{\beta_2 P_S} A_{SR_1}(d_{SR_1}, f) h_{SR_1} s_3(2t+1) \\ & + \sqrt{P_{R_2}} A_{R_2R_1}(d_{R_2R_1}, f) h_{R_2R_1} \hat{s}_3(2t) + n_{R_1}(2t+1), \end{aligned} \tag{6}$$

where $s_1(2t+1)$ and $s_3(2t+1)$ are the desired signals, while $\hat{s}_3(2t+1)$ is the interference, which results in a degraded performance. We assume that the indirect link has worse channel conditions than the two direct links. Therefore, the modem R_1 employs successive interference cancellation (SIC) to first decode $s_3(2t+1)$, followed by $s_1(2t+1)$ by treating $\hat{s}_3(2t)$ as interference. Therefore the received signal-to-interference-noise ratio (SINR) at R_1 is given by

$$\gamma_{R_1} = \frac{\beta_1 A_{SR_1}^2(d_{SR_1}, f) h_{SR_1}^2 \rho_S}{A_{R_2R_1}^2(d_{R_2R_1}, f) h_{R_2R_1}^2 \rho_{R_2} + 1}, \tag{7}$$

where $\rho_S \triangleq P_S/\sigma^2$, and $\rho_k \triangleq P_k/\sigma^2$, $k = \mathrm{R}_1, \mathrm{R}_2$. Considering the transmission from S to D and R_1, the SINR at R_1 for the detection of $s_3(2t+1)$ from (6) is given by

$$\gamma_{D,S\to R_1} = \frac{\beta_2 A^2_{SR_1}\big(d_{SR_1},f\big)h^2_{SR_1}\rho_S}{\mathcal{A}+1}, \tag{8}$$

where

$$\mathcal{A} \triangleq \beta_1 A^2_{SR_1}\big(d_{SR_1},f\big)h^2_{SR_1}\rho_S + A^2_{R_2R_1}\big(d_{R_2R_1},f\big)h^2_{R_2R_1}\rho_{R_2}.$$

Similarly, the SINR at D for the transmission from S-D is given by

$$\gamma_{D,S\to D^{s_3}} = \frac{\beta_2 A^2_{SD}(d_{SD},f)h^2_{SD}\rho_S}{\beta_1 A^2_{SD}(d_{SD},f)h^2_{SD}\rho_{R_1}+1}. \tag{9}$$

1) WITHOUT DIRECT LINK TO D

Considering that there is no direct link between S and D (as shown in Fig. 1), the received signal at D is given by

$$z_D(2t+1) = A_{R_2D}\big(d_{R_2D},f\big)h_{R_2D}x_{R_2}(2t+1) + n_D(2t+1). \tag{10}$$

For the relayed transmission from R_2 to D, the received SINR at D is given by

$$\gamma_{D,R_2\to D} = A^2_{R_2D}\big(d_{R_2D},f\big)h^2_{R_2D}\rho_{R_2}. \tag{11}$$

2) WITH DIRECT LINK TO D

As shown in Fig. 2, let us consider a direct link between S and D. During the time slot $(2t+1)$, $t = 0, 1, \ldots,$ S transmits the superimposed signal (2) to both R_1 and D. The received signal at D is given by

$$\begin{aligned} z_{D,S\to D}(2t+1) &= A_{SD}(d_{SD},f)h_{SD}x_s(2t+1) \\ &\quad + A_{R_2D}\big(d_{R_2D},f\big)h_{R_2D}x_{R_2}(2t+1) + n_D(2t+1). \end{aligned} \tag{12}$$

Substituting (2) and (3) into (12), we get

$$\begin{aligned} z_{D,S\to D}(2t+1) &= \sqrt{\beta_1 P_S}A_{SD}(d_{SD},f)h_{SD}s_1(2t+1) \\ &\quad + \sqrt{\beta_2 P_S}A_{SD}(d_{SD},f)h_{SD}s_3(2t+1) \\ &\quad + \sqrt{P_{R_2}}A_{R_2D}\big(d_{R_2D},f\big)h_{R_2D}\hat{s}_3(2t) + n_D(2t+1), \end{aligned} \tag{13}$$

For the relayed transmission from R_2 to D, the received SINR at D is given by

$$\gamma_{D,R_2\to D} = A^2_{R_2D}\big(d_{R_2D},f\big)h^2_{R_2D}\rho_{R_2}. \tag{14}$$

$$\gamma_{D,R_2\to D^{s_3}} = \frac{A^2_{R_2D}\big(d_{R_2D},f\big)h^2_{R_2D}\rho_S}{A^2_{SD}(d_{SD},f)h^2_{SD}\rho_{R_1}+1}. \tag{15}$$

Next, we consider the communication in even time slots.

B. EVEN TIME SLOTS

During the even time slot $(2t)$, $t = 0, 1, \ldots,$ S transmits the superimposed signal

$$x_s(2t) \triangleq \Big(\sqrt{\beta_1 P_S}s_2(2t) + \sqrt{\beta_2 P_S}s_3(2t)\Big), \tag{16}$$

to R_2, where $s_2(2t)$ and $s_3(2t)$ are the signals intended to R_2 and D, respectively. As mentioned earlier, The signal detected by R_2 at this time slot is forwarded to D in the next time slot. That is, R_1 forwards the decoded signal received from the previous odd time slot to R_2 and D, which is

$$x_{R_1}(2t) = \sqrt{P_{R_1}}\tilde{s}_3(2t-1), \tag{17}$$

where $\tilde{s}_3(2t-1)$ is the detected signal at R_1. The received signals at R_2 is given by

$$\begin{aligned} z_{R_2}(2t) &= A_{SR_2}\big(d_{SR_2},f\big)h_{SR_2}x_s(2t) \\ &\quad + A_{R_1R_2}\big(d_{R_1R_2},f\big)h_{R_1R_2}x_{R_1}(2t) + n_{R_2}(2t). \end{aligned} \tag{18}$$

The received signal at R_2 is obtained by substituting (16) and (17) into (18) as

$$\begin{aligned} z_{R_2}(2t) &= \sqrt{\beta_1 P_S}A_{SR_2}\big(d_{SR_2},f\big)h_{SR_2}s_2(2t) \\ &\quad + \sqrt{\beta_2 P_S}A_{SR_2}\big(d_{SR_2},f\big)h_{SR_2}s_3(2t) \\ &\quad + \sqrt{P_{R_1}}A_{R_1R_2}\big(d_{R_1R_2},f\big)h_{R_1R_2}\tilde{s}_3(2t-1) + n_{R_2}(2t). \end{aligned} \tag{19}$$

Similar to the previous case, R_2 employs SIC to first decode $s_3(2t)$, and then $s_2(2t)$ by treating $\tilde{s}_3(2t-1)$ as interference. The detected and re-encoded signal $\hat{s}_3(2t)$ will be forwarded to D at the next odd time slot as in (3). Therefore, the SINR at R_2 is

$$\gamma_{R_2} = \frac{\beta_1 A^2_{SR_2}\big(d_{SR_2},f\big)h^2_{SR_2}\rho_S}{A^2_{R_1R_2}\big(d_{R_1R_2},f\big)h^2_{R_1R_2}\rho_{R_1}+1}. \tag{20}$$

The SINR at R_2 for the transmission from S to D and R_2, and the detection of $s_3(2t)$ from (19) is given by

$$\gamma_{D,S\to R_2} = \frac{\beta_2 A^2_{SR_2}\big(d_{SR_2},f\big)h^2_{SR_2}\rho_S}{\mathcal{B}+1}, \tag{21}$$

where

$$\mathcal{B} \triangleq \beta_1 A^2_{SR_2}\big(d_{SR_2},f\big)h^2_{SR_2}\rho_S + A^2_{R_1R_2}\big(d_{R_1R_2},f\big)h^2_{R_1R_2}\rho_{R_2},$$

and the SINR at D is equivalent to (9).

1) WITHOUT DIRECT LINK TO D

The received signal at D is given by

$$z_D(2t) = A_{R_1D}\big(d_{R_1D},f\big)h_{R_1D}x_{R_1}(2t) + n_D(2t), \tag{22}$$

For the relayed transmission from R_1 to D, the received SINR at D is given by

$$\gamma_{D,R_1\to D} = A^2_{R_1D}\big(d_{R_1D},f\big)h^2_{R_1D}\rho_{R_1}. \tag{23}$$

2) WITH DIRECT LINK TO D

The received signal at D is given by

$$z_{D,S\to D}(2t) = A_{SD}(d_{SD},f)h_{SD}x_s(2t) + A_{R_1D}\big(d_{R_1D},f\big)h_{R_1D}x_{R_1}(2t) + n_D(2t), \quad (24)$$

where $n_k(2t), k = \mathrm{R}_2, \mathrm{D}$ denotes the Bernoulli-Gaussian noise. Similar to the previous case, the received signal at D is obtained by substituting (16) and (17) into (24) as

$$z_{D,S\to D}(2t) = \sqrt{\beta_1 P_S}A_{SD}(d_{SD},f)h_{SD}s_2(2t) + \sqrt{\beta_2 P_S}A_{SR_2}\big(d_{SR_2},f\big)h_{SR_2}s_3(2t) + \sqrt{P_{R_1}}A_{R_1R_2}\big(d_{R_1R_2},f\big)h_{R_1R_2}\tilde{s}_3(2t-1) + n_D(2t). \quad (25)$$

For the relayed transmission from R_1 to D, the received SINR at D is given by

$$\gamma_{D,R_1\to D} = A^2_{R_1D}\big(d_{R_1D},f\big)h^2_{R_1D}\rho_{R_1}. \quad (26)$$

$$\gamma_{D,R_1\to D^{s_3}} = \frac{A^2_{R_1D}\big(d_{R_1D},f\big)h^2_{R_1D}\rho_{R_1}}{A^2_{SD}(d_{SD},f)h^2_{SD}\rho_{R_1}+1} \quad (27)$$

III. SUM RATE ANALYSIS

In this section, we provide an analysis on the sum rate and the overall outage probability for the considered three user PLC network, both without and with direct link to D. We first consider the sum rate in the following subsection.

A. ACHIEVABLE RATES AND SUM RATE

Note that the achievable rate at D is given by

$$C_D = (1-p)C_{B,D} + pC_{I,D} \quad (28)$$

where $C_{B,D}$ and $C_{I,D}$ represent the capacities of the corresponding PLC channels in the presence of AWGN only, and a mixture of Gaussian and impulsive noises, respectively. As shown in (6) and (19), S transmits superimposed NOMA signals on the direct links SR_1, SR_2 and SD, which has an interference term due to the signals decoded at R_2 and R_1, respectively. We assume that the signal intended to D is perfectly decoded and canceled at R_1 and R_2. The achievable rate for the direct-link receiver R_k is given by

$$C_k = \frac{1}{2}\log_2\left(1+\frac{\beta_1 A_k(d_k,f)h^2_k\rho_S}{1+A_{\bar{k}}\big(d_{\bar{k}},f\big)h^2_{\bar{k}}\rho_l}\right), \quad (29)$$

where $l = \mathrm{R}_2, \mathrm{R}_1$, $k = S\mathrm{R}_1, S\mathrm{R}_2$ and $\bar{k} = \mathrm{R}_2\mathrm{R}_1, \mathrm{R}_1\mathrm{R}_2$. Obtaining an expression for the average sum rate is difficult. In the following, we consider the scenarios without and with direct links to D separately, and in each case describe a lemma which gives an expression for the corresponding approximate average sum rate. Later in Section V, we show that these approximations are tight.

B. WITHOUT DIRECT LINK TO D

Recall that in this scenario, D receives signals forwarded from R_1 and R_2 at both odd- and even-numbered time slots. Since R_1 and R_2 operate in the decode and forward mode to transmit the signal s_3 in odd and even time slot, the achievable rate from S to D through R_1 is given by [22]

$$C_{R_1D} = \frac{1}{2}\log_2\big(1+\min\big(\gamma_{D,S\to R_1},\gamma_{D,R_1\to D}\big)\big). \quad (30)$$

Likewise, the achievable data rate for the relayed transmission from the S to D through R_2 is given by

$$C_{R_2D} = \frac{1}{2}\log_2\big(1+\min\big(\gamma_{D,S\to R_2},\gamma_{D,R_2\to D}\big)\big). \quad (31)$$

Proposition 1: The approximate expressions for C_{R_1D}, C_{R_2D} and the sum rate of the three user cooperative NOMA network without a direct link to D are given by

$$C_{R_1D} = \left(\frac{\mu_D^{(R_1)}}{2\log_e(2)}\right),\ C_{R_2D} = \left(\frac{\mu_D^{(R_2)}}{2\log_e(2)}\right), \quad (32)$$

$$C_{sum} = \frac{(\mu_{R_1}+\mu_{R_2}+\mu_D^{(R_1)}+\mu_D^{(R_2)})}{2\log_e(2)}. \quad (33)$$

Proof: See Appendix A. ■

C. WITH DIRECT LINK TO D

Recall that in this case, D receives the signals from S as well as signals which are forwarded from R_1 and R_2, at both odd- and even-numbered time slots. Since R_1 operates in the decode and forward mode to transmit the signal $s_3(2t+1)$, the achievable rate from S to D through R_1 is given by [22]

$$C_{SD,R_1} = \frac{1}{2}\log_2\big(1+\min\big(\gamma_{D,S\to R_1},\gamma_{D,S\to D^{s_3}}\big)\big). \quad (34)$$

Likewise, the achievable data rate for the relayed transmission from the S to D through R_2 is given by

$$C_{SD,R_2} = \frac{1}{2}\log_2\big(1+\min\big(\gamma_{D,S\to R_2},\gamma_{D,S\to D^{s_3}}\big)\big). \quad (35)$$

Proposition 2: The approximate expressions for C_{SD,R_1}, C_{SD,R_2} and the sum rate of the three user cooperative NOMA network with a direct link to D are given by

$$C_{SD,R_1} = \left(\frac{\mu_D^{(SR_1)}}{2\log_e(2)}\right),\ C_{SD,R_2} = \left(\frac{\mu_D^{(SR_2)}}{2\log_e(2)}\right), \quad (36)$$

$$C_{sum} \approx \frac{(\mu_{R_1}+\mu_{R_2}+\mu_D^{(SR_1)}+\mu_D^{(SR_2)})}{2\log_e(2)}. \quad (37)$$

Proof: The proof is similar to the proof of Proposition 1 given in Appendix A, and is skipped for brevity. ■

D. OPTIMAL POWER ALLOCATION

Now, we discuss an optimization problem to find the optimal power allocation coefficient $\beta_1 \in (0, 1)$ that maximizes the sum rate. The problem is formulated as

$$\max_{\beta_1} \; C_{sum} \quad \text{s.t.} \;\; 0 < \beta_1 < 1. \tag{38}$$

We subsequently show through simulations in Section V that the problem in (38) is concave in β_1. Note that finding an expression for the optimal β_1 in the above optimization problem is hard, for both with and without direct link cases. Therefore, we propose the following constrained optimization problem for a simpler case when the distances between the source to both relays are equal, and a minimum rate requirement on each communication link is imposed [23]. The modified optimization problem for the case of without direct link to D is formulated as:

$$\begin{aligned} \max_{\beta_1} \;\; & C_{sum} \\ \text{s.t.} \;\; & \beta_2 > \beta_1, \\ & C_{SR_1} \geq r_1, \;\; C_{R_1D} \geq r_3, \\ & \beta_1 > 0, \;\; \beta_2 > 0, \;\; \beta_1 + \beta_2 = 1. \end{aligned} \tag{39}$$

Similarly, a corresponding optimization problem can be formulated for the case with direct link to D as well. In both cases, it is interesting to note that the optimal β_1 values are equal. The following proposition discusses the solution to the optimal β_1 for the case of no direct link. The details for the other case are similar and are omitted for brevity.

Proposition 3: When $d_{SR_1} = d_{SR_2}$, the optimal value of β_1 which is the solution to the optimization problem in (39) for the case of without direct link to D is given by

$$\beta_1^* = \frac{\alpha_1 + \alpha_1 A_{R_2R_1}^2 \left(d_{R_2R_1}, f\right) h_{R_2R_1}^2 \rho_{R_2}}{A_{SR_1}^2 \left(d_{SR_1}, f\right) h_{SR_1}^2 \rho_S}. \tag{40}$$

Proof: See Appendix B. ∎

Note that the solution in (40) corresponds to the scenario where the constraint $C_{SR_1} \geq r_1$ is satisfied with equality, and C_{R_1D} is maximized. Such a scheme is desirable in practice.

IV. OUTAGE PROBABILITY ANALYSIS

In this subsection, we derive the expressions for outage probabilities at R_1, R_2 and D. Let the thresholds on SINRs for a given requirements on the data rate at R_1, R_2 and D for symbols s_1, s_2 and s_3 be denoted by α_1, α_2 and α_3, respectively. First, the outage at R_1 occurs if R_1 fails to decode either of the symbol s_1 or s_3, which was sent from SR_1 in the odd time slot. Therefore, the outage probability at R_1 is expressed as

$$P_{\text{out}}^{(R_1)} = P\left\{\gamma_{R_1} < \alpha_1 \text{ or } \gamma_{R_1} < \alpha_3\right\}. \tag{41}$$

To derive an expression for (41), we employ the technique discussed in [11], which can be summarized as next. We skip the mathematical details for brevity. Following the properties 1)-3) of a lognormal distribution discussed in Appendix A, it can be shown that the outage at R_1 is the approximate cumulative distribution function (CDF) of another lognormal distribution, which is given by

$$P_{\text{out}}^{(R_1)} \approx \frac{1}{2} \, \text{erfc}\left(\frac{-\ln(\max(\alpha_1, \alpha_3)) + \mu_{R_1}}{\sqrt{2}\sigma_{R_1}}\right), \tag{42}$$

where μ_{R_1} and σ_{R_1} are obtained using (53) and (54). Further, outage at R_2 occurs if R_2 fails to decode either of the symbol s_2 or s_3, following which we get

$$P_{\text{out}}^{(R_2)} = Pr\left\{\gamma_{R_2} < \alpha_2 \text{ or } \gamma_{R_2} < \alpha_3\right\}, \tag{43}$$

$$\approx \frac{1}{2} \, \text{erfc}\left(\frac{-\ln(\max(\alpha_2, \alpha_3)) + \mu_{R_2}}{\sqrt{2}\sigma_{R_2}}\right), \tag{44}$$

using the same set of arguments as before. In the following, we describe two propositions, which characterize the outage probability at the destination for without and with direct link to D.

A. WITHOUT DIRECT LINK TO D

Proposition 4: The outage probability at D for without the direct link is given by (46) in the bottom of the page.

Proof: See Appendix C. ∎

Consequently, the overall outage probability for the scenario without a direct link to D is given by

$$P_{\text{out}} = P_{\text{out}}^{(R_1)} P_{\text{out}}^{(R_2)} P_{\text{out}}^{(D)}. \tag{47}$$

As mentioned earlier, we show that the derived expressions are tight through Monte Carlo simulations in Section V.

B. WITH DIRECT LINK TO D

Proposition 5: The outage probability at D with a direct link is given by (49) given in the bottom of next page.

Proof: The outage at *D* occurs when *D* fails to decode the symbol s_3 from both the links S and R_1 in odd time slot,

$$P_{\text{out}}^{(D)} = Pr\left\{\gamma_{D,S\to R_1} < \alpha_3 \text{ or } \gamma_{D,S\to R_2} < \alpha_3\right\} \tag{45}$$

$$\approx \left(\frac{1}{2}\left[\text{erfc}\left(\frac{-\ln(\alpha_3) + (\mu_D^{(R_1)})}{\sqrt{2}(\sigma_D^{(T_1)})}\right) + \text{erfc}\left(\frac{-\ln(\alpha_3) + (\mu_D^{(R_2)})}{\sqrt{2}(\sigma_D^{(T_2)})}\right)\right] - \frac{1}{4}\left[\text{erfc}\left(\frac{-\ln(\alpha_3) + (\mu_D^{(R_1)})}{\sqrt{2}(\sigma_D^{(T_1)})}\right)\text{erfc}\left(\frac{-\ln(\alpha_3) + (\mu_D^{(R_2)})}{\sqrt{2}(\sigma_D^{(T_2)})}\right)\right]\right) \tag{46}$$

and S and R_2 in even time slot. The proof is similar to the proof of Proposition 4 given in Appendix C, and is skipped for brevity. ■

In this case, the overall outage probability is given as

$$P_{\text{out}} = P_{\text{out}}^{(R_1)} P_{\text{out}}^{(R_2)} P_{\text{out}}^{(SD)}. \tag{50}$$

C. OPTIMAL POWER ALLOCATION

Now, we discuss an optimization problem to find the optimal power allocation coefficient $\beta_1 \in (0, 1)$ that minimizes the overall outage probability. This is an alternative way to calculate β_1. The problem is formulated as

$$\begin{aligned} \min_{\beta_1} \ & P_{\text{out}} \\ \text{s.t.} \ & \beta_2 > \beta_1, \\ & \beta_1 > 0, \ \beta_2 > 0, \ \beta_1 + \beta_2 = 1. \end{aligned} \tag{51}$$

Even in this case, obtaining an expression for the optimal value of β_1 is hard, for both with and without direct link cases. However, we discuss the convexity of the problem (51) in Section V, following which the optimal β_1 can be obtained using numerical evaluation.

V. SIMULATION RESULTS

In this section, we present a study through Monte Carlo simulations to corroborate our analysis on the sum rate and outage probability. The PLC cable attenuation model is considered to be $A_i(d_i, f) = \exp(-\eta d_i)$, for $i \in \{\text{SD}, \text{SR}_1, \text{SR}_2, \text{R}_1\text{D}, \text{R}_2\text{D}, \text{R}_1\text{R}_2\}$, where $\eta = a_0 + a_1 f^m$ is the attenuation factor, a_0 and a_1 are constants determined from measurements as $a_0 = 9.4 \times 10^{-3}$, $a_1 = 4.2 \times 10^{-7}$ and $f = 30$ MHz is the center frequency, $m = 0.7$ is the exponent of the attenuation factor [12]. Unless specified otherwise, $\beta_1 = 0.1$, $\mu = 5$, $\sigma = 0.1$, $d_{SR_1} = 300$ m, $d_{R_1R_2} = d_{R_2R_1} = 1000$ m, $d_{SR_2} = d_{R_1D} = d_{R_2D} = d_{DR_1} = d_{DR_2} = (d_{SR_1} + 100)$ m, $\alpha_1 = \alpha_2 = \alpha_3 = 2^{2r} - 1$ and $r = 2$ bps/Hz.

Fig. 3 and Fig. 4 show the effect of the Bernoulli-Gaussian noise impulsive component parameter p on the sum rate and overall outage probability, for without and with direct link to D. It is observed that as the value of p increases, the performance of the system (in terms of both sum rate and outage probability) deteriorates, which translates to the inherent impulsive nature present in the noise. Moreover, as expected, the presence of a direct link from S to D improves the sum rate and outage probability. For the rest of the results, we set $p = 0$, without loss of generality.

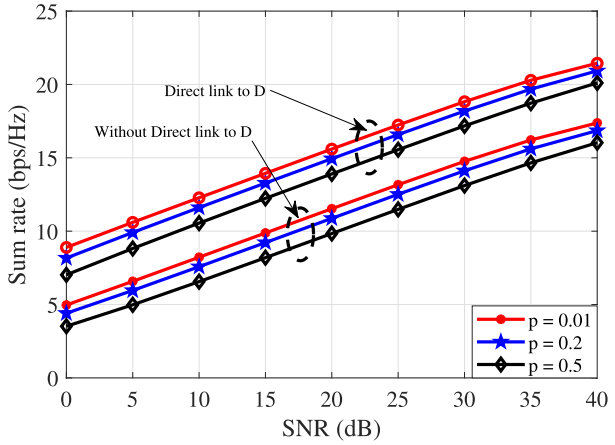

FIGURE 3. Variation of sum rate for different p values.

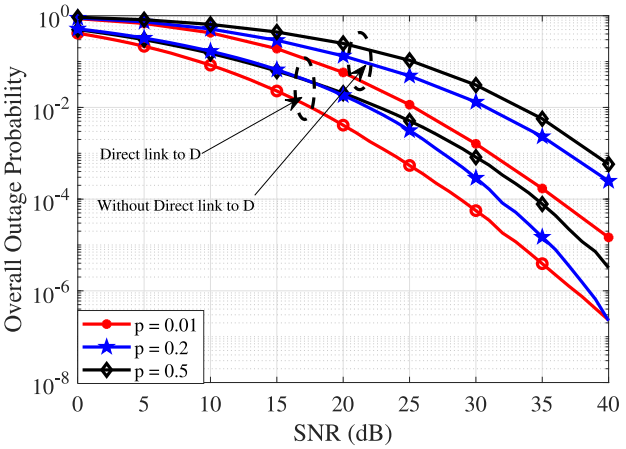

FIGURE 4. Variation of overall outage probability for different p values and $d_{SR_1} = 500$ m, $\sigma = 1$.

Fig. 5 and Fig. 6 show the sum rate performances obtained due to Monte Carlo simulations and our approximate analysis given in Section III-A, in terms of the SNR for different values of distance d_{SR_1} and d_{SD} for without direct link to D and with direct link to D, respectively. The near-perfect match between the two in both cases establishes the accuracy of our analysis. Further, as expected, the sum rate increases with SNR and decreases with an increase in d_{SR_1} and d_{SD}. Moreover, it is shown that the sum rate performance of the considered three-user network without a direct link to D is better than the three-user NOMA benchmark, which we

$$P_{\text{out}}^{(SD)} = Pr\{(\gamma_{D,S\to R_1} + \gamma_{D,S\to D^{s3}}) < \alpha_3 \text{ or } (\gamma_{D,S\to R_2} + \gamma_{D,S\to D^{s3}}) < \alpha_3\} \tag{48}$$

$$\approx \left(\frac{1}{2}\left[\text{erfc}\left(\frac{-\ln(\alpha_3) + (\mu_D^{(SR_1)})}{\sqrt{2}(\sigma_D^{(SD,T_1)})}\right) + \text{erfc}\left(\frac{-\ln(\alpha_3) + (\mu_D^{(SR_2)})}{\sqrt{2}(\sigma_D^{(SD,T_2)})}\right)\right] - \frac{1}{4}\left[\text{erfc}\left(\frac{-\ln(\alpha_3) + (\mu_D^{(SR_1)})}{\sqrt{2}(\sigma_D^{(SD,T_1)})}\right)\text{erfc}\left(\frac{-\ln(\alpha_3) + (\mu_D^{(SR_2)})}{\sqrt{2}(\sigma_D^{(SD,T_2)})}\right)\right]\right) \tag{49}$$

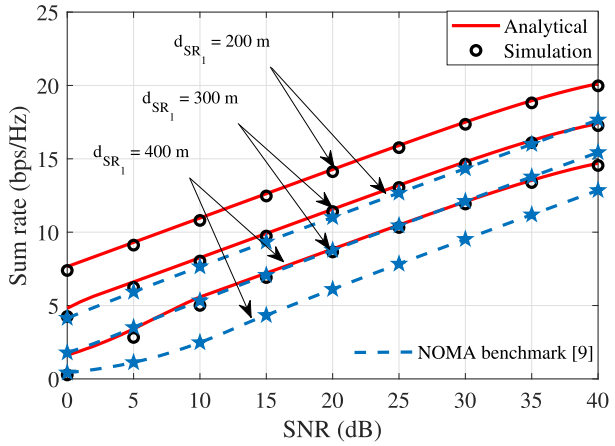

FIGURE 5. Sum rate performance comparison with simulations and approximations without direct link to D, along with NOMA benchmark.

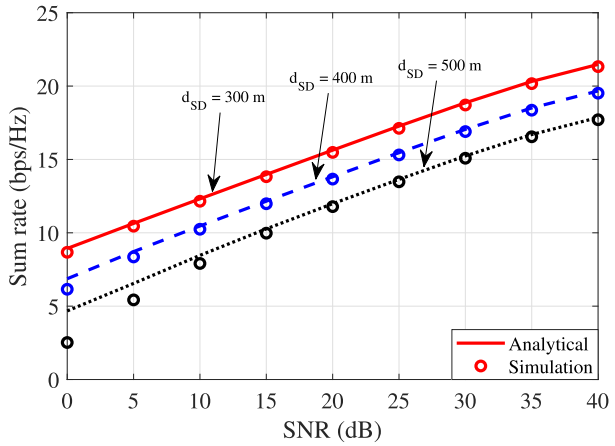

FIGURE 6. Sum rate performance comparison with simulations and approximations with a direct link to D.

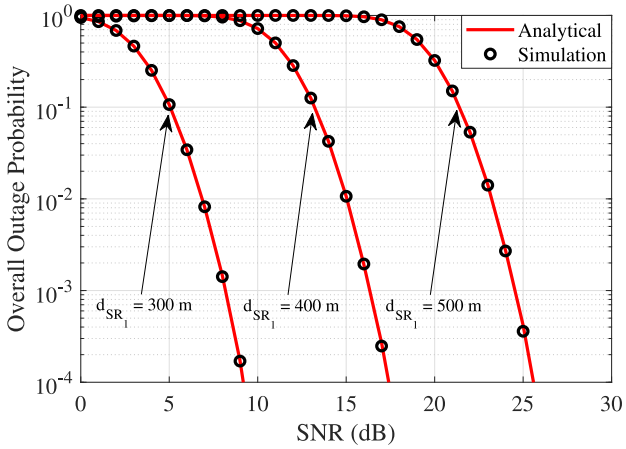

FIGURE 7. Comparison of outage probabilities obtained from simulations and approximations, without direct link to D.

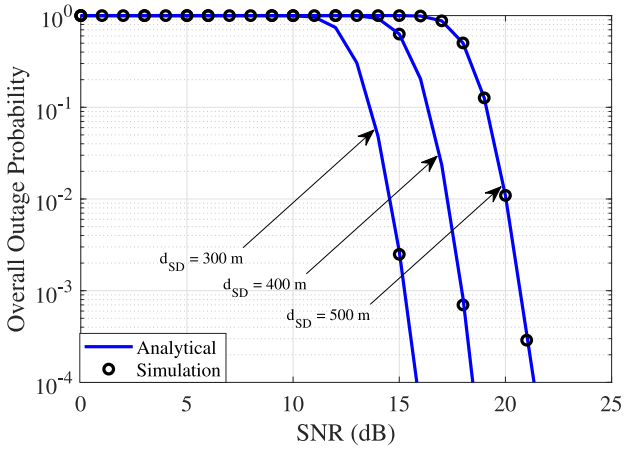

FIGURE 8. Comparison of outage probabilities obtained from simulations and approximations, with a direct link to D.

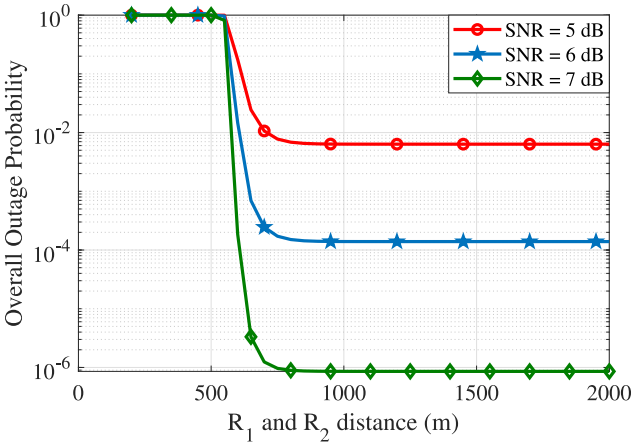

FIGURE 9. Variation of outage probability with respect to distance between R_1 and R_2, without direct link to D.

have extended from [18] to a PLC scenario. In the NOMA benchmark scheme, S sends superimposed signal to R_1 in the first time slot, which forwards the signal to D at the second slot. In the third slot, S communicates with R_2 directly. The transmit power and the power allocation coefficients of the S in the NOMA benchmark scheme are optimized and set up similar to the employed scheme.

Fig. 7 and Fig. 8 highlights the outage probabilities obtained through Monte Carlo simulations and the approximate analysis discussed in Section IV for the system models considered on Fig. 1 and Fig. 2, respectively. Even in this case, the near-perfect match between the two highlights the accuracy of our analysis. Fig. 9 shows the overall outage probability of the cooperative NOMA scheme without direct link, where as the inter-user channel distance between R_1 and R_2 increases the performance decreases and remains constant after a particular distance. The concave behavior of the sum rate with respect to the power allocation coefficient β_1 is observed in Fig. 10, as discussed in Section III. The optimal power allocation coefficients are chosen using the steepest ascent algorithm.

Fig. 11 highlights the variation and comparison of the theoretical and simulated optimal power allocation coefficient β_1^*, with respect to the SR distance and $\mu = 0.5$,

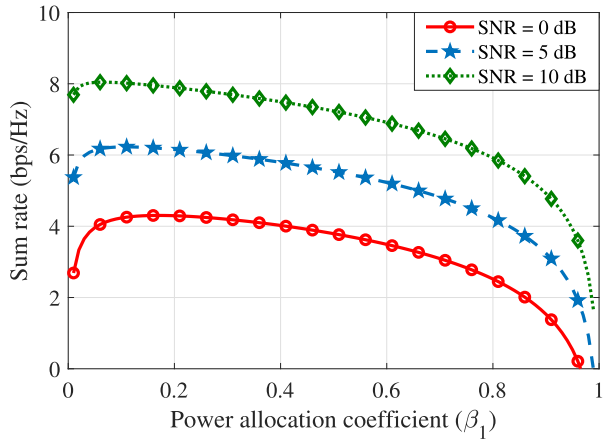

FIGURE 10. Variation of sum rate with respect to power allocation coefficient, without direct link to D.

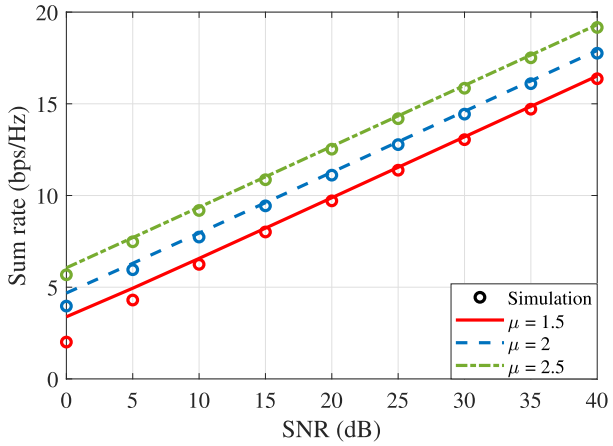

FIGURE 13. Variation and comparison of theoretical and simulated sum rates with transmit SNR, for the case of without direct link to D.

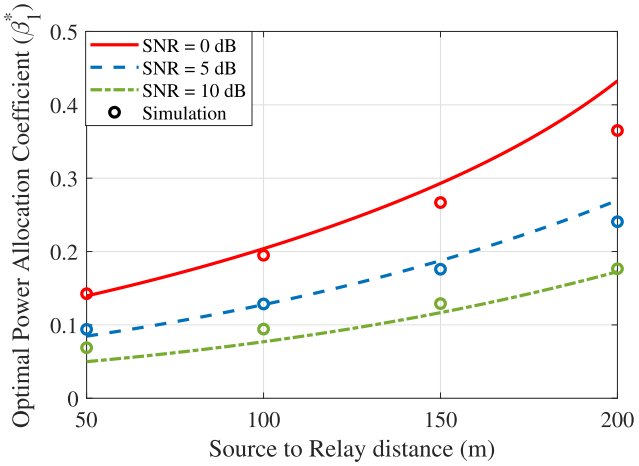

FIGURE 11. Variation and comparison of theoretical and simulated optimal power allocation coefficients, with the S-R distance for the case of without direct link to D. Here, we set parameter $\mu = 0.5$ and $r_1 = r_2 = 1$ bps/Hz.

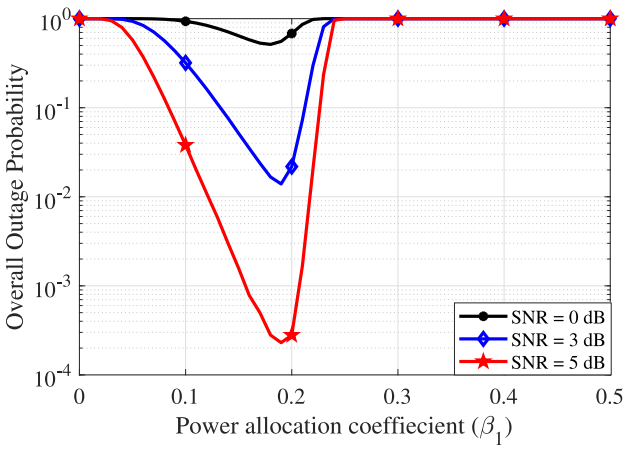

FIGURE 14. Variation of overall outage probability with β_1, for $\mu = 2$, $r_3 = 2$ bps/Hz, without direct link to D.

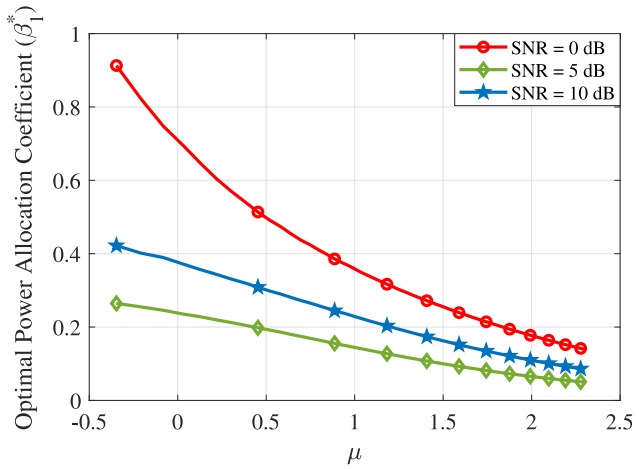

FIGURE 12. Variation of the optimal β_1 with parameter μ for the case of without direct link to D, and $r_1 = r_2 = 1$ bps/Hz.

$r_1 = r_2 = 1$ bps/Hz. The good match between simulations and theoretical values validates our analysis. Further, β_1^* increases as the SD distance increases, as expected. Fig. 12 shows the variation of the optimal β_1^* with respect to parameter μ. Since C_{sum} is directly dependent on the parameter μ, small values of β_1^* maximize the sum rate for larger values of μ. Next, Fig. 13 shows the variation of sum rate for different transmit SNR. It can be observed that there is a slight mismatch between theoretical and simulated sum rates for low values of SNR and low values of μ. This trend is expected, since the Maclaurin series expansion used in the derivation of the sum rate becomes tighter for higher values of μ. Fig. 14 highlights the convexity of the outage probability with respect to β_1, as discussed in Section IV.

Fig. 15 and Fig. 16 compares the sum rate and the overall outage probability of the three-user network for both models, i.e., without direct link to D and with direct link to D. Recall that $p = 0$. It is observed that the performance of the system with a direct link to D is higher as compared to the system for without direct link to D for the given SNR and d_{SR_1}, as expected.

Finally, we present a performance comparison of the three-user cooperative NOMA network without a direct link to D with the two-user SS-, DS-NOMA and OMA networks

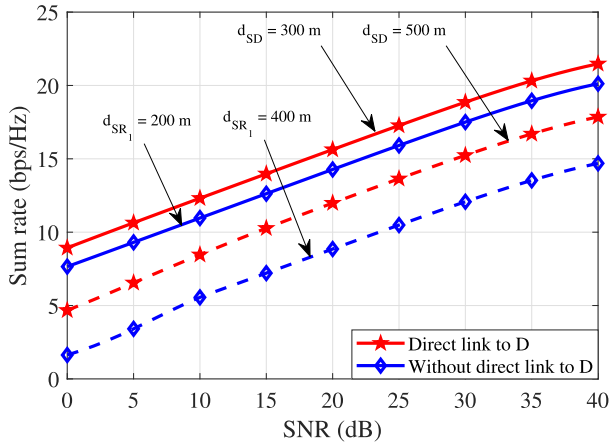

FIGURE 15. Performance comparison of average sum rates for without and with direct link to D.

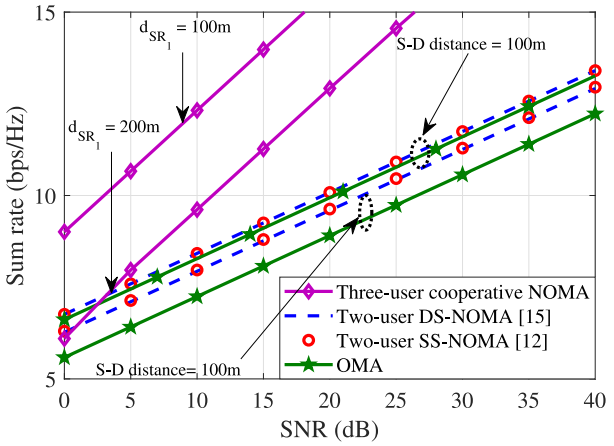

FIGURE 17. Sum rate performance comparison with single-stage and dual-stage cooperative NOMA with two users [15].

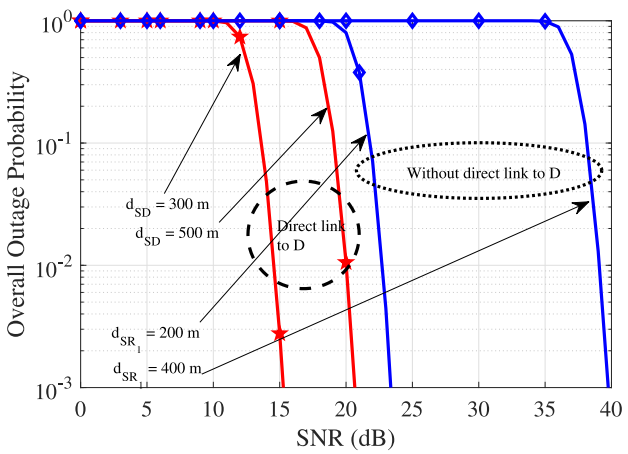

FIGURE 16. Performance comparison of overall outage probabilities for without and with direct link to D.

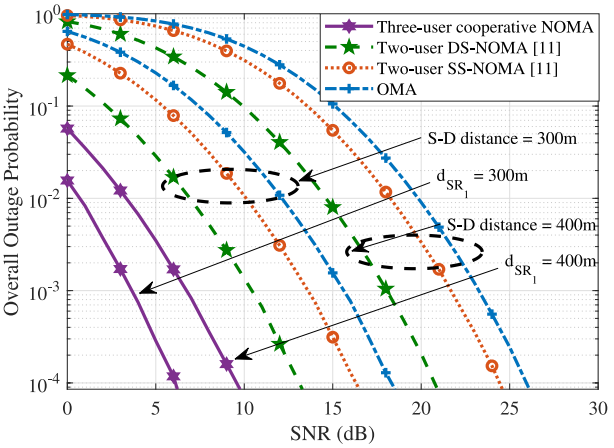

FIGURE 18. Outage probability performance comparison with single-stage and dual-stage cooperative NOMA with two users [11].

considered in [11] and [12], [15]. Fig. 17 and Fig. 18 compares the sum rate and the overall outage probability of the considered three-user network without a direct link to D, respectively. It is observed that the considered three-user network outperforms all others schemes in terms of sum rate and overall outage probability. It should be further noted that the performance comparison with a direct link to D is not included, since the performance of that case is better than that of the scenario without the direct link.

VI. CONCLUSIONS

We studied the performance of three-user cooperative NOMA for PLC, with a single source modem, two relays and a single destination modem. We derived closed form expressions for the approximate sum rates and the overall outage probability of the network, in the presence and absence of a direct link between the source and destination. We presented an analysis to find the optimal power allocation co-efficient, such that the sum rate is maximized. Further, we provided insights of the impact of the parameters such as the distance, fading and impulsive noise component on the overall on the PLC system performance, and established the accuracy of our analysis through Monte Carlo simulations. Our scheme was shown to outperform existing schemes in the literature, in terms of sum rate and outage probability.

APPENDIX A
PROOF OF PROPOSITION 1

We start by considering the rate of R_1. The cumulative distribution function (CDF) of the received SINR at R_1 is given by

$$F_{\gamma_{R_1}}(x) = P\left(\frac{\beta_1 A_{SR_2}(d_{SR_2}, f)h^2_{SR_2}\rho_S}{A_{R_1R_2}(d_{R_1R_2}, f)h^2_{R_1R_2}\rho_{R_1}+1} \leq x\right), \quad (52)$$

where, following the properties of a lognormal distribution, it is easy to see that $h^2_{SR_1} \sim \mathcal{LN}(2\mu_{SR_1}, 4\sigma^2_{R_2D})$, and $h^2_{R_2R_1} \sim \mathcal{LN}(2\mu_{R_2R_1}, 4\sigma^2_{R_2R_1})$. Now, recall that if $H_i \sim \mathcal{LN}(\mu_i, \sigma_i^2)$ and $H_j \sim \mathcal{LN}(\mu_j, \sigma_j^2)$, then

1) $kH_i \sim \mathcal{LN}(\mu_i + \ln k, \sigma_i^2)$, for $k \in \mathbb{R}^+$,
2) $\frac{H_i}{H_j} \sim \mathcal{LN}(\mu_l, \sigma_l^2)$; $\mu_l = \mu_i - \mu_j$, and $\sigma_l = \sigma_i + \sigma_j$, and
3) $H_l = H_i + H_j$ can be well-approximated by another lognormal distribution, with parameters μ_l and σ_l^2,

which can be calculated as [24],

$$\mu_l = \frac{1}{2}\log \mathbb{E}\left[H_l^{-2}\right] - 2\log \mathbb{E}\left[H_l^{-1}\right], \quad (53)$$

$$\sigma_l^2 = \log \mathbb{E}\left[H_l^{-2}\right] - 2\log \mathbb{E}\left[H_l^{-1}\right]. \quad (54)$$

where the moments $\mathbb{E}[H_l^{-1}]$ and $\mathbb{E}[H_l^{-2}]$ can be calculated either through simulations, or numerically as

$$\mathbb{E}\left[H_l^{-1}\right] = \int_0^\infty \int_0^\infty (h_i + h_j)^{-1} f_{H_i}(h_i) f_{H_j}(h_j) dh_i dh_j,$$

$$\mathbb{E}\left[H_l^{-2}\right] = \int_0^\infty \int_0^\infty (h_i + h_j)^{-2} f_{H_i}(h_i) f_{H_j}(h_j) dh_i dh_j,$$

where $f_{H_1}(h_1)$ and $f_{H_2}(h_2)$ are the PDFs of H_i and H_j. Using the aforementioned properties, we obtain the CDF of γ_{R_1} using (52) as

$$F_{\gamma_{R_1}}(x) = \frac{1}{2}\,\text{erfc}\left(\frac{-\ln x + \mu_{R_1}}{\sqrt{2}\sigma_{R_1}}\right), \quad (55)$$

where μ_{R_1} and σ_{R_1} are evaluated using (53) and (54), respectively. Thus, the average achievable rate at the link SR_1 is given by

$$C_{SR_1} = \int_0^\infty \frac{\log_2(1+x)}{\sqrt{8\pi\sigma_{R_1}^2 x}} \exp\left(-\frac{-\ln x + \mu_{R_1}}{\sqrt{2}\sigma_{R_1}}\right)^2 dx. \quad (56)$$

Changing the variable $\ln x = t$ in (56), we get

$$C_{SR_1} = \int_{-\infty}^\infty \frac{\log_2(1+e^t)}{\sqrt{8\pi\sigma_{R_1}^2}} \exp\left(-\frac{-t + \mu_{R_1}}{\sqrt{2}\sigma_{R_1}}\right)^2 dx \quad (57)$$

Further, we employ the Maclaurin series expansion of the exponential function inside the integral in (57), and evaluate the integral by truncating the series to the first term. We obtain the expression for the average rate as:

$$C_{SR_1} \approx \left(\frac{\mu_{R_1}}{2\log_e(2)}\right). \quad (58)$$

Similarly, the average rate of the link S-R_2 is given by

$$C_{SR_2} \approx \left(\frac{\mu_{R_2}}{2\log_e(2)}\right), \quad (59)$$

where μ_{R_2} is obtained from (53). Next, we consider the links connecting the D modem. Similar to what is considered in [19], we assume that $\{\min(\gamma_{D,S\to R_1}, \gamma_{D,R_1\to D})\} \approx \gamma_{D,S\to R_1}$ to evaluate C_{R_1D}, and $\{\min(\gamma_{D,S\to R_2}, \gamma_{D,R_2\to D})\} \approx \gamma_{D,S\to R_2}$ to evaluate C_{R_2D}. As a result, expressions of C_{R_1D} and C_{R_2D} given in (30) and (31) can be approximated as

$$C_{SD,R_1} \approx \frac{1}{2}\log_2(1+\gamma_{D,S\to R_1}). \quad (60)$$

$$C_{SD,R_2} \approx \frac{1}{2}\log_2(1+\gamma_{D,S\to R_2}). \quad (61)$$

APPENDIX B
PROOF OF PROPOSITION 3

We follow the technique described in [23]. Recall that we have $d_{SR_1} = d_{SR_2}$. In this case, it is easy to show that C_{sum} as a function of β_1 can be written as

$$C_{sum} \triangleq f(\beta_1) = C_{SR_1} + C_{R_1D}. \quad (62)$$

Now, the optimization problem in (39) can be rewritten as:

$$\max_{\beta_1} \; f(\beta_1)$$
$$\text{s.t.} \quad \left[\frac{(2^{2r_1}-1)}{\mathcal{K}_1}\right] \le \beta_1 \le \left[\frac{(\mathcal{K}_2 - (2^{2r_3-1}))}{\mathcal{K}_2(1+(2^{2r_3-1}))}\right], \quad (63)$$

where

$$\mathcal{K}_1 \triangleq \frac{A_{SR_1}^2(d_{SR_1}, f) h_{SR_1}^2 \rho_S}{A_{R_2R_1}^2(d_{R_2R_1}, f) h_{R_2R_1}^2 \rho_{R_2} + 1}, \quad (64)$$

$$\mathcal{K}_2 \triangleq \frac{\mathcal{K}_3}{\mathcal{K}_3 + \mathcal{K}_4}, \quad (65)$$

$$\mathcal{K}_3 \triangleq A_{SR_2}^2(d_{SR_2}, f) h_{SR_2}^2 \rho_S, \quad (66)$$

$$\mathcal{K}_4 \triangleq A_{R_1R_2}^2(d_{R_1R_2}, f) h_{R_1R_2}^2 \rho_{R_2} + 1. \quad (67)$$

Further, note that the lower and upper bounds on β_1 in (63) must be less than 0.5, in order to satisfy the principle of NOMA [23]. Using this, we obtain the following conditions for the threshold rates r_1 and r_3 in (39), defined in terms of α_1 and α_3 given by

$$\alpha_1 \triangleq 2^{2r_1} - 1 \le \mathcal{K}_1, \quad (68)$$

$$\alpha_3 \triangleq 2^{2r_3-1} > \mathcal{K}_2. \quad (69)$$

The derivative of the cost function $f(\beta_1)$ is calculated as

$$\frac{df(\beta_1)}{d\beta_1} \triangleq \mathcal{D}_{\beta_1} f(\beta_1) = \frac{\mathcal{K}_1\mathcal{K}_4 - \mathcal{K}_3}{\ln(2)(\mathcal{K}_1\beta_1 + 1)(\mathcal{K}_3\beta_1 + 1)}. \quad (70)$$

It is observed that the slope of the function $f(\beta_1)$ has a positive value, since $|h_{SR_1}|^2 > |h_{R_1D}|^2$. Since $f(\beta_1)$ is a strictly increasing function, it is maximized when β_1 is equal to the upper bound $[\frac{(\mathcal{K}_2-(2^{2r_3-1}))}{\mathcal{K}_2(1+(2^{2r_3-1}))}]$. This implies that the optimal solution corresponds to the power allocated for signal at D – which is far away from S – to meet the minimum transmission rate requirement r_3. The remaining power is allocated to R_1 which is near to the source, which can meet the minimum transmission rate r_1. However, in practice, it may be desirable to maximize the rate at the far user, while guaranteeing the minimum rate requirement at the near user. To derive this solution, we consider the following. The solution for the optimization problem (63) is obtained from the KKT conditions, which are given as follows:

1) $\mathcal{D}_{\beta_1} g(\beta_1) + \lambda_1 \mathcal{D}_{\beta_1}(\frac{\alpha_1}{\mathcal{K}_1} - \beta_1) + \lambda_2 \mathcal{D}_{\beta_1}(\beta_1 - \frac{\mathcal{K}_2-\alpha_3}{\mathcal{K}_2(1+\alpha_3)}) = 0,$
2) $(\frac{\alpha_1}{\mathcal{K}_1} - \beta_1)\lambda_1 = 0,$
3) $(\beta_1 - \frac{\mathcal{K}_2-\alpha_3}{\mathcal{K}_2(1+\alpha_3)})\lambda_2 = 0,$
4) $\frac{\alpha_1}{\mathcal{K}_1} - \beta_1 \le 0,$
5) $\beta_1 - \frac{\mathcal{K}_2-\alpha_3}{\mathcal{K}_2(1+\alpha_3)} \le 0,$

6) $0 < \beta_1 < \frac{1}{2}$,
7) $\lambda_1, \lambda_2 \geq 0$,

where $g(\beta_1) = -f(\beta_1) \leq 0$ and λ_1, λ_2 are the Lagrange multipliers for the constraints $C_{SR_1} \geq r_1$ and $C_{R_1D} \geq r_3$ respectively. For $\lambda_1 > 0$ and $\lambda_2 > 0$, both KKT conditions 2) and 3) must be satisfied. Setting $\lambda_1 > 0$ and $\lambda_2 = 0$, the optimal β_1 can be obtained from conditions 1) and 2) as

$$\beta_1^* = \frac{\alpha_1}{\mathcal{K}_1}. \tag{71}$$

This solution corresponds to maximizing the rate at D, by equating the rate constraint on R_1. For completeness, setting $\lambda_2 > 0$ and $\lambda_1 = 0$ gives the optimal value of β_1 following condition 3), which corresponds to maximizing the rate at R_1, by equating the rate constraint at D.

APPENDIX C
PROOF OF PROPOSITION 4

The outage at D occurs when D fails to decode the symbol s_3 from either of the links from R_1 or R_2. That is,

$$P_{\text{out}}^{(D)} = Pr\{\gamma_{D,S\to R_1} < \alpha_3 \text{ or } \gamma_{D,S\to R_2} < \alpha_3\}, \tag{72}$$

$$= \left(\left[\mathrm{F}_{D,S\to R_1}(\alpha_3) + \mathrm{F}_{D,S\to R_2}(\alpha_3)\right] - \left[\mathrm{F}_{D,S\to R_1}(\alpha_3)\mathrm{F}_{D,S\to R_2}(\alpha_3)\right]\right), \tag{73}$$

where $\mathrm{F}_k(\alpha)$ denotes the CDF of the random variable γ_k evaluated at a point $\alpha \in \mathbb{R}$. Next, to derive the outage probability of D, we need to obtain the CDFs of $\gamma_{D,S\to R_1}$ and $\gamma_{D,S\to R_2}$. To this end, both random variables $\gamma_{D,S\to R_1}$ and $\gamma_{D,S\to R_2}$ are approximated as lognormal random variables with parameters obtained by following (53) and (54), given in Appendix A. These parameters are calculated using the properties 1)-3) described in Appendix A. Substituting the corresponding parameters in the CDFs and simplifying gives the required result.

REFERENCES

[1] A. Pittolo and A. M. Tonello, "A synthetic statistical MIMO PLC channel model applied to an in-home scenario," *IEEE Trans. Commun.*, vol. 65, no. 6, pp. 2543–2553, Jun. 2017.

[2] M. Tlich, A. Zeddam, F. Moulin, and F. Gauthier, "Indoor power-line communications channel characterization up to 100 MHz—part I: One-parameter deterministic model," *IEEE Trans. Power Del.*, vol. 23, no. 3, pp. 1392–1401, Jul. 2008.

[3] D. Wang, Y. Song, and X. Wang, "Channel modeling of broadband powerline communications," in *Proc. ICCSN*, Dec. 2017, pp. 427–430.

[4] A. M. Tonello and F. Versolatto, "New results on top-down and bottom-up statistical PLC channel modeling," in *Proc. Third Workshop Power Line Commun. its App.*, Oct. 2009, pp. 11–14.

[5] R. Ramesh, B. Sushma, S. Gurugopinath, and R. Muralishankar, "Capacity analysis of a narrowband powerline communication channel under impulsive noise," in *Proc. COMSNETS*, May 2019, pp. 272–277.

[6] S. P. Herath, N. H. Tran, and T. Le-Ngoc, "Optimal signaling scheme and capacity limit of PLC under Bernoulli-Gaussian impulsive noise," *IEEE Trans. Power Del.*, vol. 30, no. 1, pp. 97–105, Feb. 2015.

[7] R. K. Ahiadormey, P. Anokye, H.-S. Jo, C. Song, and K.-J. Lee, "Secrecy outage analysis in NOMA power line communications," *IEEE Commun. Lett.*, vol. 25, no. 5, pp. 1448–1452, May 2021.

[8] R. K. Ahiadormey, P. Anokye, H.-S. Jo, and K.-J. Lee, "Performance analysis of two-way relaying in cooperative power line communications," *IEEE Access*, vol. 7, pp. 97264–97280, 2019.

[9] X. Cheng, R. Cao, and L. Yang, "Relay-aided amplify-and-forward Powerline communications," *IEEE Trans. Smart Grid*, vol. 4, no. 1, pp. 265–272, Mar. 2013.

[10] Y. Saito, Y. Kishiyama, A. Benjebbour, T. Nakamura, A. Li, and K. Higuchi, "Non-orthogonal multiple access (NOMA) for cellular future radio access," in *Proc. VTC Spring*, 2013, pp. 1–5.

[11] R. Ramesh, S. Gurugopinath, and S. Muhaidat, "Outage performance of relay-assisted single- and dual-stage NOMA over power line communications," *IEEE Access*, vol. 9, pp. 86358–86368, 2021.

[12] K. M. Rabie, B. Adebisi, E. H. G. Yousif, H. Gacanin, and A. M. Tonello, "A comparison between orthogonal and non-orthogonal multiple access in cooperative relaying power line communication systems," *IEEE Access*, vol. 5, pp. 10118–10129, 2017.

[13] W. Duan, X.-Q. Jiang, M. Wen, J. Wang, and G. Zhang, "Two-stage superposed transmission for cooperative NOMA systems," *IEEE Access*, vol. 6, pp. 3920–3931, 2018.

[14] S. M. R. Islam, N. Avazov, O. A. Dobre, and K. Kwak, "Power-domain non-orthogonal multiple access (NOMA) in 5G systems: Potentials and challenges," *IEEE Commun. Surveys Tuts.*, vol. 19, no. 2, pp. 721–742, Secondquarter 2017.

[15] K. M. Rabie, B. Adebisi, A. M. Tonello, S. Yarkan, and M. Ijaz, "Two-stage non-orthogonal multiple access over power line communication channels," *IEEE Access*, vol. 6, pp. 17368–17376, 2018.

[16] A. Samir, M. Elsayed, A. A. El-Banna, K. Wu, and B. M. Elhalawany, "Performance of NOMA-based dual-hop hybrid Powerline-wireless communication systems," *IEEE Trans. Veh. Technol.*, pp. 1–1, 2022.

[17] R. Ramesh and S. Gurugopinath, "Sum rate analysis of cooperative NOMA over dual-hop wireless-power line communication," in *Proc. INDICON*, Dec. 2021, pp. 1–6.

[18] J. Kim and I. Lee, "Non-orthogonal multiple access in coordinated direct and relay transmission," *IEEE Commun. Lett.*, vol. 19, no. 11, pp. 2037–2040, Nov. 2015.

[19] Z. Fang, J. Hu, Y. Lu, and W. Ni, "Three-user cooperative NOMA transmission," *IEEE Wireless Commun. Lett.*, vol. 9, no. 4, pp. 465–469, Apr. 2020.

[20] U. Bhuyan and S. Rao, "Performance analysis of three user cooperative NOMA," in *Proc. TENCON 2021 -. IEEE Region 10 Conf. (TENCON)*, Dec. 2021, pp. 57–62.

[21] M. De Piante and A. M. Tonello, "On impedance matching in a power-line-communication system," *IEEE Trans. Circuits Syst. II*, vol. 63, no. 7, pp. 653–657, Jul. 2016.

[22] M. R. Bhatnagar, "On the capacity of decode-and-forward relaying over Rician fading channels," *IEEE Commun. Lett.*, vol. 17, no. 6, pp. 1100–1103, Jun. 2013.

[23] C.-L. Wang, J.-Y. Chen, and Y.-J. Chen, "Power allocation for a Downlink non-orthogonal multiple access system," *IEEE Wireless Commun. Lett.*, vol. 5, no. 5, pp. 532–535, Oct. 2016.

[24] J. C. S. S. Filho, P. Cardieri, and M. D. Yacoub, "Simple accurate lognormal approximation to lognormal sums," *IEEE Power Electron. Lett.*, vol. 41, no. 18, pp. 1016–1017, Sep. 2005.

ROOPESH RAMESH (Graduate Student Member, IEEE) received the B.E. degree in electronics and communication engineering from the Dr. Ambedkar Institute of Technology, Visvesvaraya Technological University, Bengaluru, India, in 2016, the M.Tech. degree in digital communication engineering from PES University, Bengaluru, India, in 2018. He is currently pursuing the Ph.D. degree with PES University, Bengaluru, India. His current research interests include cooperative powerline communications, NOMA, and MIMO systems.

SANJEEV GURUGOPINATH (Senior Member, IEEE) is a Professor with the Department of Electronics and Communication Engineering, PES University, Bengaluru. His current research interests include beyond 5G communication systems, powerline communications, underwater acoustics, and speech signal processing. He was a co-recipient of the Best Paper Awards at IEEE INDICON 2016, IEEE ICEECCOT 2019, IEEE CONECCT 2020, IEEE CONECCT 2021, IEEE IEMECON 2021, and IEEE INDICON 2022.

SAMI MUHAIDAT (Senior Member, IEEE) received the Ph.D. degree in electrical and computer engineering from the University of Waterloo, Waterloo, in 2006. From 2007 to 2008, he was an NSERC Postdoctoral Fellow with the Department of Electrical and Computer Engineering, University of Toronto, Canada. From 2008 to 2012, he was an Assistant Professor with the School of Engineering Science, Simon Fraser University, Burnaby, BC, Canada. He is currently a Professor with Khalifa University and an Adjunct Professor with Carleton University, Canada. His research interests include advanced digital signal processing techniques for wireless communications, RIS, 5G and beyond, MIMO, optical communications, the IoT with emphasis on battery-free devices, and machine learning. He served as a Senior Editor and an Editor for the IEEE COMMUNICATIONS LETTERS, an Editor for the IEEE TRANSACTIONS ON COMMUNICATIONS, and an Associate Editor for the IEEE TRANSACTIONS ON VEHICULAR TECHNOLOGY. He is currently an Area Editor of the IEEE TRANSACTIONS ON COMMUNICATIONS and the Lead Guest Editor for the Special Issue on Large-Scale Wireless Powered Networks With Backscatter Communications of the IEEE OPEN JOURNAL OF THE COMMUNICATIONS SOCIETY.